

# Evolution of spectral properties along the O(6)-U(5) transition in the interacting boson model. I. Level dynamics

Stefan Heinze<sup>1</sup>, Pavel Cejnar<sup>2</sup>, Jan Jolie<sup>1</sup>, Michal Macek<sup>2</sup>

<sup>1</sup>*Institute of Nuclear Physics, University of Cologne, Zùlpicherstrasse 77, 50937 Cologne, Germany*

<sup>2</sup>*Faculty of Mathematics and Physics, Charles University,*

*V Holešovičkách 2, 180 00 Prague, Czech Republic*

(Dated: July 10, 2018)

We investigate the evolution of quantal spectra and the corresponding wave functions along the  $[O(6)-U(5)]\supset O(5)$  transition of the interacting boson model. The model is integrable in this regime and its ground state passes through a second-order structural phase transition. We show that the whole spectrum as a function of the Hamiltonian control parameter, as well as structures of all excited states, exhibit rather organized and correlated behaviors, that provide deeper insight into the nature of this transitional path.

PACS numbers: 21.60.Fw, 21.10.Re, 05.45.Mt

## I. INTRODUCTION

Properties of the interacting boson model (IBM) [1] in transitional regimes between various dynamical symmetries have been extensively studied mainly in connection with zero-temperature quantum phase transitions [2, 3]. In any of such transitions, the structures of the ground state and few low-lying states change abruptly (for the system size tending to infinity) at a certain critical point, located on the way between the two dynamical-symmetry limits, see, e.g., Refs. [4, 5, 6, 7, 8, 9]. This behavior finds experimental evidence (in a finite- $N$  approximation) in observed variations of nuclear shapes in some isotopic or isotonic chains of nuclei.

The IBM phase transitions are of the first order, except the isolated point of a second-order transition, which is located at the intersection of borders between spherical and deformed, and between prolate and oblate shapes in the parameter space [4, 5, 6]. To pass this point, one commonly starts from the O(6) dynamical symmetry and proceeds to U(5) via the line of unbroken O(5) dynamical symmetry. The deformed-to-spherical second-order phase transition on this path manifests itself as a non-analytic but continuous change of the ground-state deformation, in contrast to the discontinuous changes observed along the other (even infinitely close) transitional paths. This type of phase structure of the parameter space agrees with the classical Landau theory of thermodynamic phase transitions, that is applicable at zero temperature if the role of thermodynamic variables is taken by the model control parameters [7, 8], and with catastrophe theory [2, 5].

The above-mentioned  $[O(6)-U(5)]\supset O(5)$  transitional path differs from the others also in that it does not destroy the integrability of the Hamiltonian. Due to the underlying O(5) dynamical symmetry [10], the integrals of motions along the whole transition form a complete set of commuting operators and the Hamiltonian eigenproblem can be solved analytically [11, 12]. This was used for an explicit calculation of some second-order phase-transitional observables [13]. Recent studies of the O(6)-

U(5) transitional path were also based on the concepts of the E(5) critical-point dynamical symmetry [14, 15] and the quasidynamical symmetry [16].

The ultimate mechanism that is on the deepest level responsible for the occurrence of ground-state phase transitions of various orders in quantum many-body systems remains unclear. The distinction between the IBM first- and second-order phase transitions, e.g., was shown [9] to be connected with different densities of unavoided energy crossings (branch points) in the complex-extended parameter space, which in the  $N \rightarrow \infty$  limit accumulate infinitely close to critical points on the real axes (in analogy with similar behaviors of complex zeros of partition functions in thermodynamic phase-transitional systems). However, many questions—among them the role of integrability in the process of dynamical-symmetry breaking—still remain open.

The present work contributes to the mapping of this relatively new territory of physics by studying in detail various spectral observables associated with the integrable phase-transitional path in the IBM. In particular, we investigate the evolution of energies and wave functions of individual Hamiltonian eigenstates with zero angular momentum along the whole  $[O(6)-U(5)]\supset O(5)$  line. It is shown that this transitional class of IBM exhibits rather peculiar features.

We will combine two totally different, but mutually related general approaches: (i) the theory of level dynamics, initiated by Pechukas and Yukawa [17], also known as the dynamical Coulomb-gas analogy, and (ii) the semiclassical theory of quantal spectra, represented by the Gutzwiller and Berry-Tabor trace formulas [18]. Results obtained by applying both these approaches will be presented in two parts: approach (i) is discussed in the present article (Part I), which gives numerical results on level dynamics, while approach (ii) will be used in the following article [19] (Part II).

The Pechukas-Yukawa theory describes the dynamics of individual levels and the interaction matrix elements via a set of coupled differential equations, where the varying Hamiltonian control parameter plays the role of time.

It enables one to understand the evolution of spectral observables with the control parameter (including eventual phase transitions) in a more intuitive way, using the parallel with a classical ensemble of charged particles moving in one dimension.

The trace formulas, on the other hand, describe a snapshot of the energy spectrum at each fixed value of the control parameter (“time”) by expressing the quantum density of states (as a function of energy) through properties of periodic orbits in the classical limit of the system. Since both methods (i) and (ii) translate the original problem to the classical language, they often provide deeper understanding of specific behaviors observed on the quantum level. Also in our case, the most significant features of the IBM in the  $[O(6)-U(5)] \supset O(5)$  transitional regime will be elucidated by both kinds of classical concepts involved in the above approaches.

The plan for this part of the paper is the following: In Section II we will briefly describe the quantum Hamiltonian under study, its integrals of motions and phase-transitional features. Section III presents numerical results on the level dynamics and their interpretation in the framework of the Pechukas-Yukawa theory. The accompanying changes in the structure of wave functions are then discussed in Section IV. Finally, Section V contains partial conclusions of this part of the paper.

## II. QUANTUM HAMILTONIAN

The interacting boson model [1] describes shapes and collective motions of atomic nuclei in terms of an ensemble of  $N$  interacting  $s$  and  $d$  bosons with angular momenta 0 and 2, respectively. To analyze the evolution of properties of this model along the  $O(6)$ - $U(5)$  transitional path, we adopt the Hamiltonian

$$\hat{H}(\eta) = a \left[ -\frac{1-\eta}{N^2} (\hat{Q} \cdot \hat{Q}) + \frac{\eta}{N} \hat{n}_d \right], \quad (1)$$

where the dimensionless control parameter  $\eta \in [0, 1]$  changes the proportion of both competing terms and drives the system between the  $O(6)$  ( $\eta = 0$ ) and  $U(5)$  ( $\eta = 1$ ) dynamical symmetries. The operator  $\hat{n}_d = (d^\dagger \cdot \tilde{d}) = N - \hat{n}_s$  represents the  $d$ -boson number, while  $\hat{Q} \equiv \hat{Q}_0^{(2)} = [s^\dagger \tilde{d} + d^\dagger \tilde{s}]^{(2)}$  stands for the  $O(6)$ - $U(5)$  quadrupole operator. The energy scale is set by an arbitrary factor  $a$ , which in the following will be fixed at the value  $a = 1$  MeV.

Hamiltonian (1) is a special case of a more general Hamiltonian of the same form, but with the quadrupole operator given by  $\hat{Q}_\chi^{(2)} = \hat{Q}_0^{(2)} + \chi [d^\dagger \tilde{d}]^{(2)}$ , where  $\chi \in [-\frac{\sqrt{7}}{2}, +\frac{\sqrt{7}}{2}]$  is an additional control parameter. Eq. (1), where  $\chi = 0$ , can be decomposed [20] into a linear combination of Casimir invariants corresponding to the  $O(6)$ ,  $O(5)$ ,  $O(3)$ , and  $U(5)$  algebras, with no admixture of  $SU(3)$ ,  $\overline{SU(3)}$ , and  $\overline{O(6)}$  invariants, i.e., describes the

$[O(6)-U(5)] \supset O(5)$  transitional line in the extended Casen triangle [6].

The above Hamiltonian can also be rewritten as

$$\hat{H}(\eta) = (1-\eta)\hat{H}(0) + \eta\hat{H}(1) = \hat{H}_0 + \eta\hat{V}, \quad (2)$$

which is the form well known from various studies of quantum phase transitions. Assuming  $a = 1$ , we obtain

$$\hat{H}_0 = -\frac{1}{N^2} (\hat{Q} \cdot \hat{Q}), \quad (3)$$

$$\hat{V} = \frac{1}{N} \hat{n}_d + \frac{1}{N^2} (\hat{Q} \cdot \hat{Q}). \quad (4)$$

The evolution of Hamiltonian (2) with  $\eta$  can be treated in a perturbative way since  $\hat{H}(\eta + \delta\eta) = \hat{H}(\eta) + \delta\eta \hat{V}$ . Note that the powers of  $N$  in denominators of Eqs. (1), (3) and (4) guarantee convenient scaling of the Hamiltonian with variable boson number  $N \gg 1$ .

It can be easily shown that for Hamiltonian (2) the ground-state average  $\langle V \rangle_\eta \equiv \langle \psi_1(\eta) | \hat{V} | \psi_1(\eta) \rangle = \frac{dE_1(\eta)}{d\eta}$  [where  $E_1(\eta)$  and  $|\psi_1(\eta)\rangle$  are the ground-state energy and wave function, respectively] is a nonincreasing function of  $\eta$ . Therefore, if  $\hat{V}$  is nonnegative—as in our specific case, see Eq. (4)—then an instantaneous satisfaction of  $\langle V \rangle_{\eta_c} = 0$  at some critical point  $\eta_c$  implies that the average gets fixed for all  $\eta \geq \eta_c$ , freezing both the energy and wave function of the ground state. At this point, the system may exhibit (for  $N \rightarrow \infty$ ) a ground-state phase transition of order  $\kappa \geq 2$ . If the second derivative of energy changes discontinuously from a value  $\frac{d^2 E_1(\eta)}{d\eta^2} = \frac{d\langle V \rangle_\eta}{d\eta} < 0$  at  $\eta = \eta_{c-}$  to zero at  $\eta = \eta_{c+}$ , the transition is of the second order. Higher-order transitions [2, 3] would require additional constraints, namely  $\frac{d^k \langle V \rangle_\eta}{d\eta^k} |_{\eta_{c-}} = 0$  for  $k < \kappa$ .

It is not difficult to see that for the specific Hamiltonian in Eq. (1) the ground-state average of  $\hat{V}$  indeed interpolates between a positive value at  $\eta = 0$  and zero at  $\eta = 1$ . However, the phase-transitional scenario is generically allowed only in the limit of infinite Hilbert-space dimensions, thus  $N \rightarrow \infty$ , when the ground-state energy as a function of  $\eta$  may acquire nonanalytic character. The asymptotic critical point is located at  $\eta_c = \frac{4}{5} = 0.8$ . At this point, the deformed ground-state configuration, given by a mixed-boson condensate  $|\psi_1\rangle \propto (s^\dagger + \beta_{\text{gs}} d_0^\dagger)^N |0\rangle$ , changes into the pure  $s$ -boson condensate,  $|\psi_1\rangle \propto (s^\dagger)^N |0\rangle$ , characterizing the spherical  $U(5)$  phase. In the left vicinity of the critical point the ground-state “deformation parameter”  $\beta_{\text{gs}}$  drops to zero as  $\beta_{\text{gs}} \propto \sqrt{\eta_c - \eta}$  [7] and the corresponding value of  $\langle V \rangle_\eta$  behaves according to  $N \rightarrow \infty$  asymptotic formula  $\langle V \rangle_\eta \propto (\eta_c - \eta)$  [9]. Thus both  $\beta_{\text{gs}}$  and  $\langle V \rangle_\eta$  can be considered as order parameters describing a second-order quantum phase transition,  $\kappa = 2$ , with critical exponents  $\frac{1}{2}$  and 1, respectively.

The limits  $\hat{H}(0)$  and  $\hat{H}(1)$  of Eq. (1) possess the  $O(6)$  and  $U(5)$  dynamical symmetries, respectively. Since the dynamical-symmetry Hamiltonians are constructed using

solely observables “in involution” (the Casimir invariants of the respective algebraic chain), they are always integrable [21]. Moreover, because the  $O(5)$  dynamical symmetry underlying both  $O(6)$  and  $U(5)$  limits is not broken in the transitional regime, the integrability of Hamiltonian (1) is preserved for all values of  $\eta$  [20, 22]. Indeed, one can find five mutually commuting integrals of motion, the same number as the dimension of the classical configuration space (given by two geometric parameters and three Euler angles [23]). Four of these integrals can be associated with the following quantum numbers: energy  $E_i(\eta)$  given by the Hamiltonian  $\hat{H}(\eta)$ , squared angular momentum  $l(l+1)$  represented by  $\hat{L}^2$  (where  $\hat{L} = [d^\dagger \tilde{d}]^{(1)}$ ), its projection  $m$  determined from  $\hat{L}_z$ , and the seniority  $v$  defined through the  $v(v+3)$  eigenvalue of the  $O(5)$  Casimir invariant [1]:

$$\hat{C}_2[O(5)] = \frac{1}{5}(\hat{L} \cdot \hat{L}) + 2(\hat{T}_3 \cdot \hat{T}_3) \quad (5)$$

(where  $\hat{T}_3 = [d^\dagger \tilde{d}]^{(3)}$ ). The fifth integral of motion, connected with the so-called missing label  $\tilde{n}_\Delta$  of the  $O(5) \supset O(3)$  reduction, is not given explicitly, but its existence is guaranteed by the fact that there must be five independent commuting operators in the complete set, so the Hamiltonian (which is made of four of them) commutes with the fifth one [21]. Note that in this paper we will only consider the set of states with zero angular momentum,  $l = 0$ .

### III. EIGENVALUE DYNAMICS

#### A. Pechukas-Yukawa equations

Drawing the dependence of all individual level energies  $E_i(\eta)$  for Hamiltonian (2) on the control parameter, one obtains a picture containing  $n$  continuous curves that resemble trajectories  $x_i(t)$  of an ensemble of particles in one dimension. The motion of levels is described by a set of Hamilton-type first-order differential equations associated with a gas of particles interacting via two-dimensional Coulomb force:

$$\frac{d^2 E_i}{d\eta^2} = 2 \sum_{j(\neq i)} \frac{|V_{ij}|^2}{E_i - E_j} \quad (6)$$

(analogous to  $\frac{d^2 x_i}{dt^2} = \frac{1}{2\pi\epsilon_0} \sum_{j(\neq i)} \frac{q_i q_j}{x_i - x_j}$ ). In contrast to the ordinary gas dynamics, however, the “product charge”  $|V_{ij}|^2 = |\langle \psi_i(\eta) | \hat{V} | \psi_j(\eta) \rangle|^2 \leftrightarrow q_i q_j \equiv Q_{ij}$  cannot be factorized and varies as the “time”  $\eta \leftrightarrow t$  elapses. Thus the product charges (alias interaction matrix elements) are also dynamical variables, subject to specific evolution, and the system’s phase space is larger than  $2n$ . Besides Eq. (6) we have

$$\frac{dV_{ij}}{d\eta} = -\frac{V_{ii} - V_{jj}}{E_i - E_j} + \sum_{k(\neq i,j)} \frac{E_i + E_j - 2E_k}{(E_i - E_k)(E_j - E_k)} V_{ik} V_{kj}. \quad (7)$$

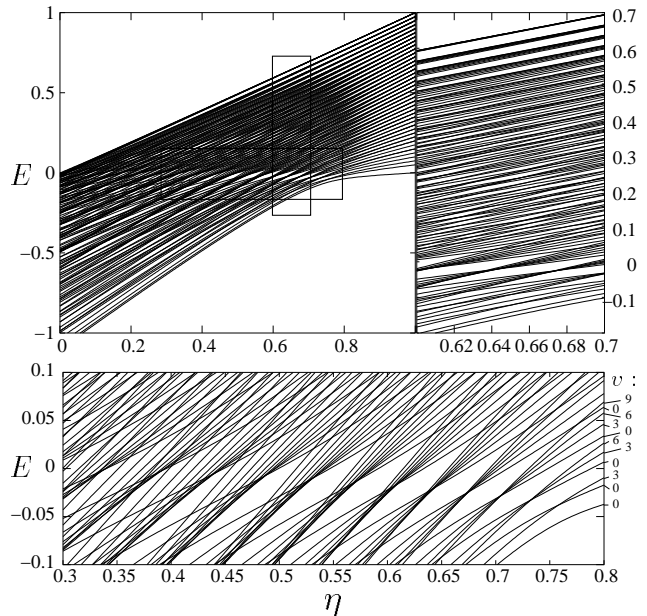


FIG. 1: Spectrum of Hamiltonian (1) with  $N = 40$  as a function of  $\eta$  for  $l = 0$  levels with all seniorities. The vertical and horizontal rectangles are expanded in the upper right and lower panels, respectively. The seniority is assigned to several levels in the lower panel.

for  $i \neq j$ , and

$$\frac{dE_i}{d\eta} = V_{ii}. \quad (8)$$

Eqs. (6)–(8) are equivalent to the well-known Pechukas-Yukawa set of equations [17], although we use here a slightly different form than the one usually found in textbooks [24]. The system described by these equations is deterministic and even integrable. If all energies and interaction matrix elements are known at a single point  $\eta$  (for instance  $\eta = 0$ ), the equations determine  $E_i$ ’s and  $V_{ij}$ ’s for all other  $\eta$  values.

Since the product charge  $|V_{ij}|^2$  in Eq. (6) is non-negative, the levels never touch each other unless their mutual interaction completely vanishes. In absence of symmetry-dictated zeros of the interaction matrix, the coincidence of simultaneous convergences  $|V_{ij}|^2 \rightarrow 0$  and  $E_{i+1} - E_i \rightarrow 0$  is extremely unlikely, which gives rise to the well-known “no-crossing” rule for level energies. The presence of symmetries, however, induces the disappearance of  $V_{ij}$ ’s for certain sets of states which, therefore, can cross. In case of Hamiltonian (1), this concerns levels with different values of angular momentum  $l$  and levels with different seniority  $v$ .

#### B. Level bunching around $E \approx 0$

In Figure 1 we show the dynamics of all levels with  $l = 0$  along the  $\eta \in [0, 1]$  path between the  $O(6)$  and

U(5) dynamical symmetries of Hamiltonian (1). The calculation was performed by numerical diagonalization of the Hamiltonian for  $N = 40$  bosons. One can observe numerous level crossings, particularly in the region around  $E \approx 0$  (the horizontal rectangle, expanded in the lower panel), which is a consequence of the unbroken O(5) dynamical symmetry of the system. Indeed, the seniority quantum numbers, as marked for few levels on the right-most side of the lower panel, differ for any pair of levels that cross at some point. We will see below that the crossings disappear after separation of levels with different seniorities into several figures.

The pattern of consecutive compressions and dilutions of the spectrum in the region around  $E \approx 0$  is one of the most apparent attributes of Fig. 1 (see the lower panel). A striking feature of this pattern is the regular sequence that characterizes the total numbers of levels involved in individual bunches: when descending from  $\eta = 0.8$  to  $\approx 0.4$ , the sequence goes like 1, 2, 3, 4, ... At first, the different seniority states seem to cross exactly at the same point (within the available numerical precision), but with  $\eta$  descending below 0.65 the higher seniorities get increasingly out of focus, and the bunching pattern becomes more and more diffuse. Nevertheless, the structure of alternating clusters and gaps extends over a wide range  $\eta \in [0.3, 0.8]$ . Secondary “interference” patterns are also visible at other energies (see the vertical rectangle of Fig. 1, extended in the upper right-hand-side panel), but these are much weaker than the main one.

The energy  $E \approx 0$ , where the bunching pattern appears, is significant because it corresponds to the local maximum at  $\beta = 0$  of the classical potential [1, 23] corresponding to Hamiltonian (1). The bunching of levels thus develops just at the value of energy where the classically accessible range of the deformation parameters,  $\beta \in [\beta_{\min}, \beta_{\max}]$ , extends due to  $\beta_{\min}$  becoming zero. The connection of the bunching pattern with the IBM classical dynamics will be elaborated in Part II of this contribution [19].

### C. Shock-wave scenario

Figure 2 demonstrates that the level bunching pattern can be deconvoluted by separating states with different seniorities. Here we show the level dynamics for  $v = 0$  (this set includes the ground state) and  $v = 18$ , with the boson number  $N = 80$ . Clearly, the  $v = 0$  levels in panel (a) form a smooth flow with a “shock wave” propagating from the top of the spectrum (at  $\eta = 0$ ) to the ground state (at  $\eta = 0.8$ ). The mutual distances  $\Delta E_i = E_{i+1} - E_i$  of individual  $v = 0$  levels as functions of  $\eta$  are shown in Figure 3(a), where we can clearly identify points of the closest approach of neighboring states as the wave propagates through the ensemble. Note that due to the energy denominator in Eq. (6), a minimal spacing of levels tends to induce maximal “force” acting on the relevant levels, which is basically the mechanism

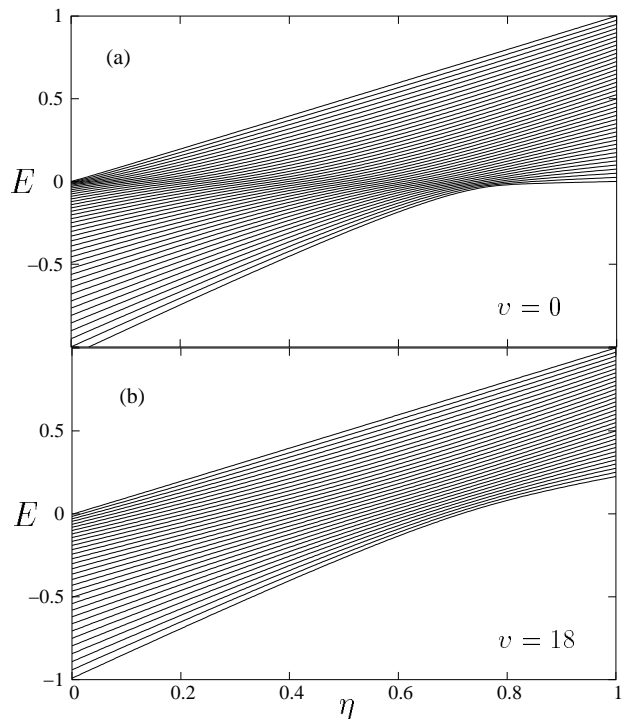


FIG. 2: Spectrum of Hamiltonian (1) with  $N = 80$  for  $l = 0$  levels with seniority  $v = 0$  (panel a) and  $v = 18$  (panel b).

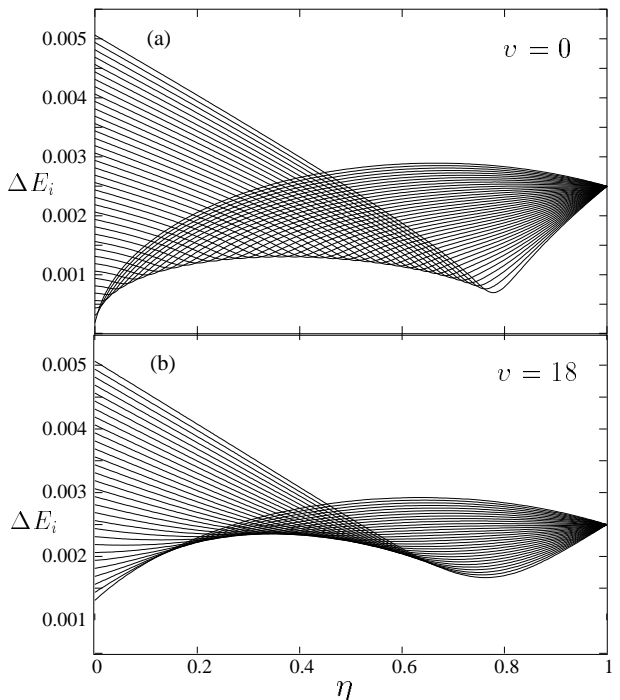


FIG. 3: Distances of neighboring levels from Fig. 2.

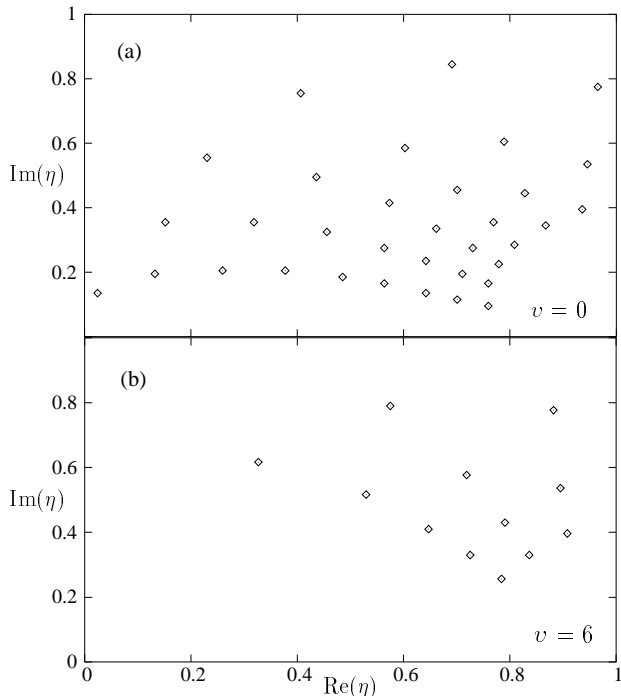


FIG. 4: Branch points of Hamiltonian (1) with  $N = 20$  for  $l = 0$  states with seniorities  $v = 0$  (panel a) and  $v = 6$  (panel b).

that keeps the wave moving. This is also why the wave initiates in the upper (densest) part of the spectrum (at  $\eta = 0$ , the distance of nearest levels linearly decreases with  $i$ , while at  $\eta = 1$  it is constant, cf. Fig. 3).

On the other hand, the dynamics of the  $v = 18$  levels, shown in panels (b) of both figures, exhibits much weaker interactions. The flow in Fig. 2(b) looks almost laminar and the minimal distances in Fig. 3(b) (still disclosing interactions) are about twice larger than in the  $v = 0$  case. It can be checked that the weakening of level interactions proceeds gradually as  $v$  increases.

The shock-wave interpretation of Fig. 2(a) is particularly appealing if used as a tentative reasoning for the ground-state phase transition at  $\eta_c = \frac{4}{5}$ . It seems that this transition results from a highly ordered sequence of structural changes that propagate from upper to lower parts of the spectrum and terminate at the ground state just at the critical point. This mechanism, however, needs to be verified by an analysis of wave functions and will be further discussed in Sec. IV.

Closely related to the regular evolution of level energies is the organized pattern of the Hamiltonian branch points in the complex plane of parameter  $\eta$  [25]. It is shown for  $N = 20$  in Figure 4 for (a)  $v = 0$  and (b)  $v = 6$ . Branch points are places in the complex-extended parameter space where two (or more) Hamiltonian complex eigenvalues become degenerate [26]. A branch point located on the real  $\eta$ -axis would imply a real crossing of

the corresponding levels, which does not typically happen (for levels with different symmetry quantum numbers). On the other hand, if a given branch point is not on, but sufficiently close to the real axis, one observes an avoided crossing of the relevant levels at the corresponding value of  $\eta$ . Remind that a sequence of such avoided crossings is significant for the “shock wave”. A cumulation of branch points in infinitesimal vicinity (for  $N \rightarrow \infty$ ) of the critical point  $\eta_c$  was recently shown [9] to constitute the essential triggering mechanism for the IBM quantum phase transitions of both orders.

For each seniority, there are altogether  $\frac{n(n-1)}{2}$  complex conjugate pairs of branch points, where  $n$  is the dimension of the given seniority subspace. Because of numerical constraints, we can only show results for moderate dimensions that correspond to the lower boson number  $N = 20$ . As can be seen in Fig. 4, branch points for both seniorities form rather regular patterns. In the  $v = 0$  case (panel a) we notice a chain of points at  $\eta < 0.8$  that approach close to the real axis. These points clearly correspond to the sequence of avoided crossings shown (for a higher boson number) in Fig. 2(a). With increasing seniority, the pattern gets more and more separated from the real axis (see the example in panel b), which results in a weakening of level interactions, as observed (for different values of  $N$  and  $v$ ) in Fig. 2(b). Note that such an organized behavior of branch points is a privilege of only the  $[O(6)-U(5)] \supset O(5)$  transitional class, where the separation of seniorities is possible (cf. Ref. [9]).

#### D. Focal point and spectral invariant

A more detailed view of Fig. 2(a) discloses that almost all  $v = 0$  levels on the  $\eta = 0$  side (except perhaps few ones on the top of the spectrum) point to a virtually sharp focus on the  $\eta = 1$  side. Indeed, an unperturbed evolution (with no mutual interactions between levels) would lead to crossing of individual lines at the point  $(\eta, E) = (1, \frac{1}{2})$ , which we call an (approximate) focal point of the  $[O(6)-U(5)] \supset O(5)$  transition.

From Eq. (8) we see that  $(\eta_f, E_f)$  will be a focal point of Hamiltonian (2) if  $\langle \psi_i(0) | \hat{H}(\eta_f) | \psi_i(0) \rangle = E_f$ , so in our particular case we have

$$\langle \psi_i(0) | \hat{n}_d | \psi_i(0) \rangle \approx \frac{N}{2}, \quad (9)$$

where  $|\psi_i(0)\rangle$  are the Hamiltonian eigenvectors with  $v = 0$  at  $\eta = 0$ . This means that the average number of  $d$ -bosons in individual  $O(6)$  eigenstates with zero seniority stays nearly constant across the whole spectrum. Figure 5(a), where the  $n_d$  average is shown explicitly along the whole  $\eta \in [0, 1]$  path for all  $v = 0$  levels with  $N = 80$ , supports this rule; see the  $\eta = 0$  limit (graphically it is difficult to distinguish, whether the convergence of all curves to the  $\frac{N}{2}$  point is exact or not, but numerical values indicate that it is only approximate). With a lower precision, the validity of the above “spectral invariant”

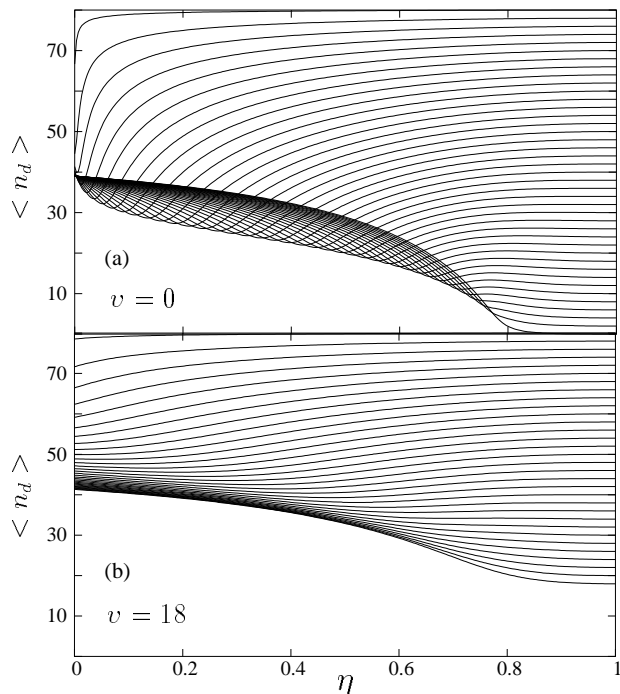


FIG. 5: The average number of  $d$ -bosons for  $v = 0$  (panel a) and  $v = 18$  (panel b) states with  $l = 0$  and  $N = 80$ .

can be extended to higher seniorities, but with increasing  $v$  there are more and more upper states that do not fit, see Fig. 5(b) that shows  $\langle n_d \rangle_i$  for the  $v = 18$  levels.

Even in the  $SU(3)-U(5)$  and  $\overline{SU}(3)-U(5)$  transitions, when  $\hat{Q}$  in Hamiltonian (1) is replaced by  $\hat{Q}_\chi$  with  $\chi = -\frac{\sqrt{7}}{2}$  or  $\chi = +\frac{\sqrt{7}}{2}$  and the seniority is not conserved, one finds a similar approximate invariant, namely  $\langle \psi_i(0) | \hat{n}_d | \psi_i(0) \rangle \approx \frac{3N}{4}$ , where  $|\psi_i(0)\rangle$  represent the  $SU(3)$  or  $\overline{SU}(3)$  eigenvectors (the complete  $l = 0$  spectrum for these transitions can be found in Ref. [8]).

Note that we first detected these invariants geometrically, from the focal points. The impact of such invariants on the level dynamics can be enormous since focal points represent an essential condition for the initial compression of the Coulomb gas, which results in stronger interactions between levels. This compression triggers the formation of the “shock wave” in the densest part of the spectrum, see Sec. III C. Therefore, the existence of an initial (exact or approximate) focal point may belong to the main causes that eventually lead to a phase transition at some point.

### E. Finite- $N$ phase transitions

Although we are dealing here with the spherical-deformed transition induced by varying parameter  $\eta$  in Hamiltonian (1), one should realize that the  $[O(6)-U(5)] \supset O(5)$  transitional path itself coincides with

the separatrix between prolate and oblate deformed phases [5, 6]. The prolate-oblate first-order phase transition for  $N \rightarrow \infty$  at any fixed value of  $\eta \in [0, \frac{4}{5})$  can be induced by varying parameter  $\chi$  in the generalized Hamiltonian of the form (1) with  $\hat{Q}$  replaced by  $\hat{Q}_\chi$ .

It is argued in Ref. [13] that the  $O(6)$  dynamical symmetry represents a special point of the IBM phase diagram where a discontinuous prolate-oblate change of the ground-state structure can be observed even for *finite* boson numbers. Indeed, if one explicitly includes the  $O(5)$  Casimir invariant (5) into the Hamiltonian with a coefficient such that the  $v = 0$  ground-state at  $(\eta, \chi) = (0, 0)$  becomes degenerate with the lowest states of other seniorities, a crossing of the ground-state configurations will occur for any value of  $N$  when passing the  $O(6)$  point in the  $\chi$ -direction.

It is easy to show that this mechanism can be extended to the whole  $\eta \in [0, \frac{4}{5})$  transitional region. The basic trick—the fact that levels with different seniorities can be made degenerate—remains the same. After subtracting the component corresponding to the  $O(5)$  Casimir invariant [20] from the general  $\chi$ -dependent Hamiltonian of the form (1), one arrives at the expression

$$\hat{H}'(\eta, \chi) \propto \frac{\eta - 1}{N^2} \left\{ (\hat{Q}_\chi \cdot \hat{Q}_\chi) - \frac{1}{2} \hat{C}_2[O(5)] \right\} + \frac{\eta}{N} \hat{n}_d, \quad (10)$$

that exhibits the desired property: For any fixed value of  $\eta$  and any finite boson number  $N$ , the ground state as a function of  $\chi$  changes discontinuously at  $\chi_c = 0$ , which thus defines the critical point for a finite- $N$  prolate-oblate phase transition.

We therefore extend the region of possible finite- $N$  phase transitions in the IBM phase diagram to the whole prolate-oblate separatrix. The key feature needed for this generalization of Ref. [13] is the integrability of the  $[O(6)-U(5)] \supset O(5)$  Hamiltonians. Note, however, that phase transitions at finite dimensions, induced by un-avoided crossings of levels involving the ground-state, represent a rather nongeneric kind of behavior, which moreover is not robust enough to survive at finite temperatures. Indeed, if the temperature increases from zero to an infinitesimally small value, nonzero populations of both levels result in a smooth dependence of the free energy on the control parameter, and the phase-transitional behavior is washed out.

### F. Bulk properties of the spectrum

It is clear that the strongest influence on a given level comes typically from its neighbors at the places of avoided crossings. Besides these binary interactions (involved in the shock-wave propagation), there exists also a component of the total force acting on each individual level that originates from the bulk of the whole ensemble. In this subsection, we will consider two global measures of this bulk component.

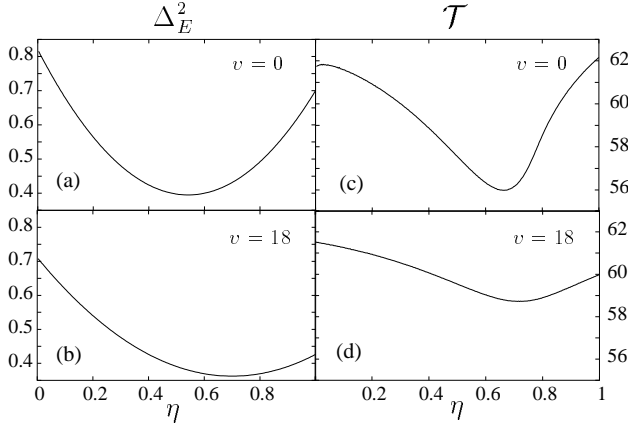


FIG. 6: The dispersion (11) of the spectrum and the kinetic energy from Eq. (13) for  $v = 0$  and 18 states, corresponding to  $l = 0$  and  $N = 80$ .

First, we consider the overall compression of all levels, represented by the energy dispersion (squared “spread”) of the spectrum,  $\Delta_E^2 = \frac{1}{n} \sum_i (E_i - \bar{E})^2$ , where  $\bar{E} = \frac{1}{n} \sum_i E_i$  is a center-of-mass energy. A straightforward calculation yields the expression

$$\Delta_E^2 = \left[ \frac{\text{Tr} \hat{H}_0^2}{n} - \frac{\text{Tr}^2 \hat{H}_0}{n^2} \right] + 2\eta \left[ \frac{\text{Tr}(\hat{H}_0 \hat{V})}{n} - \frac{\text{Tr} \hat{H}_0 \text{Tr} \hat{V}}{n^2} \right] + \eta^2 \left[ \frac{\text{Tr} \hat{V}^2}{n} - \frac{\text{Tr}^2 \hat{V}}{n^2} \right], \quad (11)$$

which shows that the spectral dispersion is a quadratic function with a minimum at

$$\eta_0 = - \frac{n \text{Tr}(\hat{H}_0 \hat{V}) - \text{Tr} \hat{H}_0 \text{Tr} \hat{V}}{n \text{Tr} \hat{V}^2 - \text{Tr}^2 \hat{V}}. \quad (12)$$

For  $\eta \approx \eta_0$ , the strengths of both terms  $\hat{H}_0$  and  $\eta \hat{V}$  of Hamiltonian (2) are comparable, so that the strongest effects of mixing take place in the surrounding region. For  $\eta \gg \eta_0$  or  $\eta \ll \eta_0$ , on the other hand, the spectrum just blows up, the Hamiltonian being dominated by  $\eta V$ .

For (a)  $v = 0$  and (b)  $v = 18$  subsets of the spectrum with  $N = 80$ , the function (11) is shown in the two left-most panels of Figure 6. We see that the  $v = 0$  levels are maximally compressed at  $\eta_0 \approx 0.56$ , i.e., in the region just before the phase transition. For higher seniorities, the minimum moves towards  $\eta_c = \frac{4}{5}$ . Let us note that a similar conclusion can be made for  $\chi \neq 0$ , when of course the seniority is not conserved and the contribution of all  $l = 0$  levels must be summed up. For  $\chi = \pm \frac{\sqrt{7}}{2}$ , for instance, the energy dispersion forms a sharp minimum directly at  $\eta_0 \approx 0.8$ .

The second quantity we will use here to characterize the bulk component of the force is the total product charge  $\mathcal{Q} = \sum_{i>j} Q_{ij} = \sum_{i>j} |V_{ij}|^2$ . It is related to

the sum

$$\underbrace{\frac{1}{2} \sum_i \left( \frac{dE_i}{d\eta} \right)^2}_{\mathcal{T}} + \underbrace{\frac{1}{2} \sum_{i \neq j} |V_{ij}|^2}_{\mathcal{V}} = \frac{1}{2} \text{Tr} \hat{V}^2 \equiv \mathcal{E}, \quad (13)$$

which is an integral of motions of the Pechukas-Yukawa model, known as the total energy [24]. Since  $\frac{d}{d\eta} \mathcal{E} = 0$ , the second term that represents the potential energy  $\mathcal{V} = \mathcal{Q}$  is at any value of  $\eta$  just a complement of the first, kinetic term  $\mathcal{T}$ . For  $\eta \gg \eta_0$  and  $\eta \ll \eta_0$  [assuming for a while  $\eta \in (-\infty, +\infty)$ ], the eigenbasis of  $\hat{H}(\eta)$  virtually coincides with the eigenbasis of  $\hat{V}$  so that  $\text{Tr} \hat{V}^2 \approx \sum V_{ii}^2 = 2\mathcal{T}$  and  $\mathcal{V} \approx 0$ . In these regions, the gas just freely expands. On the other hand, around  $\eta_0$  the kinetic and potential terms in Eq. (13) are comparable and the interaction may generate nontrivial effects.

The kinetic energy from Eq. (13) for levels with  $v = 0$  and  $v = 18$ , respectively, is shown in panels (c) and (d) of Fig. 6. In both cases, we observe a minimum of  $\mathcal{T}$  very close to the critical point; for  $v = 0$  the minimum is located at  $\eta \approx 0.67$ . This means that  $\mathcal{V} = \mathcal{Q}$  is maximal at the same place, implying the strongest overall strength of level interactions. For higher seniorities, the minimum gets shallower and moves towards  $\eta_c$ .

We saw that both the compression of the spectrum and total interaction strength are maximal in the region of control parameters around  $\eta_0$  which immediately precedes the phase transition at  $\eta_c$ . Conversely, Eq. (12) yields a reasonable rough estimate of the parameter range of a general Hamiltonian (2) where eventual phase transitions may be located.

#### IV. EIGENSTATE DYNAMICS

Besides dynamics of individual Hamiltonian eigenvalues  $E_i(\eta)$ , one can also analyze structural changes of the corresponding eigenstates  $|\psi_i(\eta)\rangle$ . These two aspects of spectral evolution are mutually correlated, since the matrix elements  $V_{ij}$ , that carry information on wave functions, belong to dynamical variables involved in Pechukas-Yukawa equations (6)–(8).

In Fig. 5, we have already seen the evolution of the average number of  $d$ -bosons,  $\langle n_d \rangle_i$ , in the  $v = 0$  and  $v = 18$  eigenstates. This information is now supplemented by Figure 7, where the  $\eta$ -dependence of the whole distribution  $P_i(n_d)$  of  $n_d$  is shown for selected  $N = 80$  Hamiltonian eigenstates, namely the  $v = 0$  states with  $i = 1, 10, 20$ , and 30 (ordered with increasing energy). For  $l$  and  $v$  fixed, the probability

$$P_i(n_d)|_\eta = \sum_{\tilde{n}_\Delta, m} |\langle n_d, v, \tilde{n}_\Delta, l, m | \psi_i(\eta) \rangle|^2 \quad (14)$$

for each  $\eta$  is determined as the projection of the state  $|\psi_i(\eta)\rangle$  onto the subspace of the  $U(5)$  eigenstates with  $n_d$  equal to the given number. In the  $U(5)$  limit, the

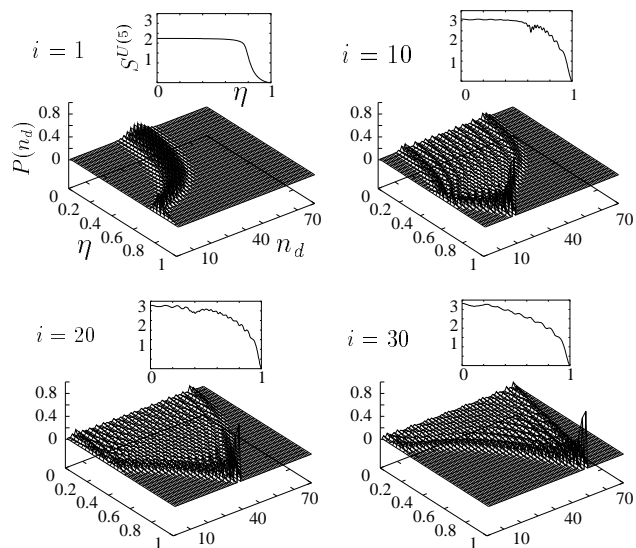


FIG. 7: The distribution of the  $d$ -boson number  $n_d$  in four  $l = v = 0$  eigenstates of Hamiltonian (1) with  $N = 80$  as a function of  $\eta$ . The insets show the corresponding U(5) wave-function entropy.

distribution is concentrated on a single value  $n_d = 2i - 2$  (with zero seniority, the value of  $n_d$  must be even), but it quickly spreads over a broad range of  $n_d$ 's as  $\eta$  decreases from 1 to 0.

Figure 7 shows four qualitatively different types of ways how this delocalization proceeds: For the ground state,  $i = 1$ , the value of  $n_d$  remains zero as far as  $\eta > \eta_c$ , and then it suddenly increases (with decreasing  $\eta$ ), forming a ridge around the average that goes approximately as  $\langle n_d \rangle_1 \propto \sqrt{\eta_c - \eta}$ , in agreement with the phase-transitional predictions; cf. Fig. 5(a). For excited states, the gradual spread of wave functions in  $n_d$  can be compared to the propagation of waves on a string. The string is initially (at  $\eta = 1$ ; the “time” is now thought to go backwards) subject to an instantaneous point perturbation and the resulting waves propagate in both  $n_d = 0$  and  $n_d = N$  directions asymmetrically. The pattern of wave propagations changes with  $i$ : for instance, the speed of the upper wave is lower for higher excited states. When the lower front of the wave reaches the  $n_d = 0$  limit, it either gets reflected (this happens for lower excited states, see the  $i = 10$  example) or stops there (for higher excited states, see  $i = 20$  and 30 cases).

It is interesting that the value of  $\eta$  where the wave reaches the lower endpoint  $n_d = 0$  coincides with the range where the “shock wave” affects the given level, see Figs. 2(a) and 3(a). This can be checked for a larger set of levels in Fig. 5(a). The dependences of individual  $n_d$  averages exhibit well-pronounced minima that correspond to the stopping or reflection of the lower wave front at  $n_d = 0$ , and reasonably coincide with the moments of passage of the shock-wave.

Also shown in the insets of Fig. 7 is the U(5) wave-function entropy,

$$S_i^{U(5)} = - \sum_{n_d=0}^N P_i(n_d) \ln P_i(n_d), \quad (15)$$

which measures the overall spread of the instantaneous eigenvector  $|\psi_i(\eta)\rangle$  in the U(5) basis [20]. Assuming a quasiuniform distribution of the  $i$ th state over a certain set of the  $\hat{n}_d$  eigenstates, one finds that the effective number of components is given by  $n_i^{\text{eff}} = \exp S_i^{U(5)}$ . This number is approximately equal to half of the width (at a given value of  $\eta$ ) of the  $n_d$  distribution corresponding to the respective level (taking into account that odd  $n_d$  values are not populated for  $v = 0$ ).

As can be seen in Fig. 7, the widths of the  $n_d$  distributions and the corresponding U(5) entropies grow with decreasing  $\eta$  as far as the distribution touches the  $n_d = 0$  limit (the level gets into the shock-wave region). After this point, the width and entropy stay approximately constant. If proceeding from the O(6) side, i.e., returning to the forward direction of “time”, we can say that the process of localization of level  $i$  in the U(5) basis starts approximately when the shock wave hits the level. This supports and further specifies the shock-wave scenario described in Sec. III C. We must stress, however, that for excited states the transition to the U(5) structure after passing the shock wave is only gradual. A sudden phase-transitional type of change is reserved for the ground state only.

As indicated by the  $i > 1$  examples in Fig. 7, the decrease of the U(5) wave-function entropy exhibits some undulations, connected with quantum interferences of the amplitudes corresponding to populations of individual  $n_d$ 's. It is surprising that vertical coordinates of the main oscillations are about constant for the whole ensemble of states. This is demonstrated in Figure 8, where we show the U(5) wave-function entropy for all (a)  $v = 0$  and (b)  $v = 18$  states ( $N = 80$ ). Clearly, if one proceeds from state to state, the undulations are shifted in  $\eta$ , but remain at about the same levels of entropy. The result is a peculiar pattern of “plateaus” present in both panels of Fig. 8. (Let us stress, however, that these plateaus are only a visual effect appearing when all entropies are drawn in the same figure.) This hints at strong correlations in the structural changes of individual eigenstates after the passage through the shock-wave region.

The most distinguished steps of the patterns in Fig. 8 are the same for both seniorities. They correspond to the effective numbers of wave-function components equal approximately to  $n_i^{\text{eff}} \approx 4.5, 7.5, 10, \text{ and } 12$ . Note that the average delocalization of a given state in a randomly chosen basis is for sufficiently high dimensions  $n$  given by  $n_{\text{GOE}}^{\text{eff}} \approx 0.48 n$  [20], which for the  $v = 0$  and  $v = 18$  subspaces yields typical saturation values of the wave-function entropy equal to  $S_{\text{GOE}} \approx 3$  and  $\approx 2.7$ , respectively. (The largest U(5) entropies in the  $\eta = 0$  limit slightly exceed the GOE values, but the latter provide



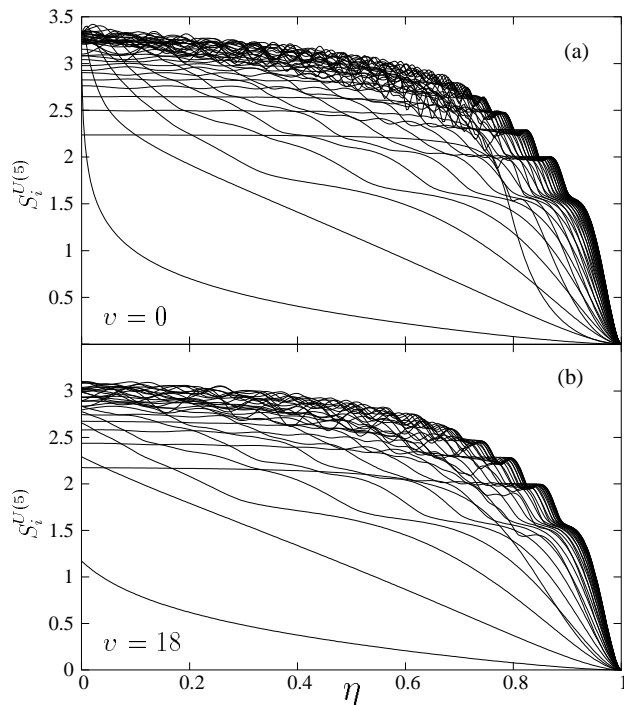


FIG. 8: The U(5) wave function entropy for all  $v = 0$  (panel a) and  $v = 18$  (panel b) eigenstates of Hamiltonian (1) with  $l = 0$  and  $N = 80$ .

reasonable estimates of averages if all states are taken into account.) We see that the system of plateaus in Fig. 8 disappear in noisy oscillations just below the respective GOE entropy values.

Let us stress that no step-like structures are observed in cumulative plots of the U(5) wave-function entropy of all  $l = 0$  states for the  $SU(3)-U(5)$  and  $\overline{SU(3)}-U(5)$  transitions. The present correlated behavior is therefore connected solely with the integrable  $\chi = 0$  region.

## V. CONCLUSIONS

We have studied dynamics of the  $l = 0$  energy levels and the corresponding eigenstates along the  $[O(6)-U(5)] \supset O(5)$  transition of the interacting boson model. Results of our numerical calculations were discussed in the framework of the Pechukas-Yukawa model, which describes the evolution of quantal spectra as one-dimensional motions of an ensemble of classical particles. Treated in this way, spectral attributes for all values of

the control parameter—including possible phase transitions at some critical points—result just from a specific “initial condition”, i.e., the set of energies and interaction matrix elements at a single *arbitrary* point  $\eta$ . Of course, particularly tempting is to consider the whole spectral evolution along  $\eta \in [0, 1]$  (and beyond) being predetermined by properties of the system in either of the two limiting dynamical symmetries.

We disclosed cooperative and highly coherent behaviors of the individual spectral constituents, i.e., level energies and wave functions corresponding to various seniorities. This may be generally linked to the integrability of the model in the present regime, namely to the possibility to separate seniorities, but we have to admit that some of the findings remain just plain observations. Further studies may still shed more light on how this all “comes about”.

The most significant cooperative effect seems to rely on the “shock-wave” mechanism, that consists in an ordered sequence of avoided crossing of levels in the region around  $E \approx 0$  and the accompanying changes of eigenstates (Secs. III C and IV). Triggered by an initial compression of the spectrum, the shock wave initiates in its densest upper part and propagates downwards to the ground state. The passage of the wave through a given state starts the gradual transfiguration of the state structure into the U(5) form. This mechanism provides a deeper insight into the process that eventually leads to the ground-state phase transition of second order.

Among the other findings we highlight the following: (a) approximate focal points of IBM spectra in transitions to the U(5) dynamical symmetry (Sec. III D), (b) possible finite- $N$  prolate-oblate phase transitions along the whole  $[O(6)-U(5)] \supset O(5)$  separatrix (Sec. III E), (c) extremes of spectral “bulk observables” in the region immediately preceding the phase transition (Sec. III F), (d) highly correlated changes of consecutive eigenstates leading to “plateaus” in the cumulative plot of U(5) wave-function entropies (Sec. IV).

In the following part of our article [19], we will focus on the interpretation of the  $E \approx 0$  pattern of level bunchings (Sec. III B) within the semiclassical theory of quantal spectra.

## Acknowledgments

We acknowledge useful discussions with R.F. Casten and J. Dobeš. This work was supported by the DFG grant no. U36 TSE 17.2.04.

[1] F. Iachello, A. Arima, *The Interacting Boson Model* (Cambridge University Press, Cambridge, UK, 1987).  
 [2] R. Gilmore, *Catastrophe Theory for Scientists and Engineers* (Wiley, New York, 1981).

[3] D.H. Feng, R. Gilmore, S.R. Deans, Phys. Rev. C **23**, 1254 (1981).  
 [4] A.E.L. Dieperink, O. Scholten, F. Iachello, Phys. Rev. Lett. **44**, 1747 (1980).

- [5] E. López-Moreno, O. Castaños, Phys. Rev. C **54**, 2374 (1996).
- [6] J. Jolie, R.F. Casten, P. von Brentano, V. Werner, Phys. Rev. Lett. **87**, 162501 (2001).
- [7] J. Jolie, P. Cejnar, R.F. Casten, S. Heinze, A. Linne-  
mann, V. Werner, Phys. Rev. Lett. **89**, 182502 (2002).
- [8] P. Cejnar, S. Heinze, J. Jolie, Phys. Rev. C **68**, 034326 (2003).
- [9] P. Cejnar, S. Heinze, J. Dobeš, Phys. Rev. C **71**, 011304(R) (2005); see also nucl-th/0501041.
- [10] A. Leviatan, A. Novoselsky, I. Talmi, Phys. Lett. B **172**, 144 (1986).
- [11] Feng Pan, J.P. Draayer, Nucl. Phys. **A636**, 156 (1998).
- [12] J. Dukelsky, S. Pittel, Phys. Rev. Lett. **86**, 4791 (2001).
- [13] J.M. Arias, J. Dukelsky, J.E. García-Ramos, Phys. Rev. Lett. **91**, 162502 (2003).
- [14] F. Iachello, Phys. Rev. Lett. **85**, 3580 (2000).
- [15] J.M. Arias, C.E. Alonso, A. Vitturi, J.E. García-Ramos, J. Dukelsky, A. Frank, Phys. Rev. C **68**, 041302(R) (2003).
- [16] D.J. Rowe, Phys. Rev. Lett. **93**, 122502 (2004); Nucl. Phys. **A745**, 47 (2004); D.J. Rowe, P.S. Turner, G. Rosensteel, Phys. Rev. Lett. **93**, 232502 (2004).
- [17] P. Pechukas, Phys. Rev. Lett. **51**, 943 (1983); T. Yukawa, *ibid.* **54**, 1883 (1985).
- [18] M.C. Gutzwiller, J. Math. Phys. **12**, 343 (1971); M.V. Berry, M. Tabor, Proc. R. Soc. Lond. **A349**, 101 (1976).
- [19] M. Macek, P. Cejnar, J. Jolie, S. Heinze, the following arXive article.
- [20] P. Cejnar, J. Jolie, Phys. Rev. E **58**, 387 (1998).
- [21] W.M. Zhang, D.H. Feng, Phys. Rep. **252**, 1 (1995).
- [22] N. Whelan, Y. Alhassid, Nucl. Phys. **A556**, 42 (1993).
- [23] R.L. Hatch, S. Levit, Phys. Rev. C **25**, 614 (1982).
- [24] H.-J. Stöckmann, *Quantum Chaos. An Introduction* (Cambridge University Press, Cambridge, UK, 1999).
- [25] W.D. Heiss, Phys. Rep. **242**, 443 (1994); I. Rotter, Phys. Rev. C **64**, 034301 (2001).
- [26] T. Kato, *Perturbation Theory of Linear Operators* (Springer-Verlag, Berlin, 1966).